15. Cruikshank, D. P., Stockton, A., Dyck, H. M., Becklin, E. E. & Macy, W. Jr *Icarus* **40**, 104–114 (1979).
16. Morrison, D. & Cruikshank, D. P. *Space Sci. Rev.* **15**, 641–739 (1974).
17. Morrison, D., Cruikshank, D. P. & Burns, J. A. in *Planetary Satellites* (ed. Burns, J.) 3–17 (University of Arizona Press, 1977).
18. Smith, B. A. *et al. Science* **215**, 504–537 (1982).
19. Harrington, R. S. & Christy, J. W. *Astr. J.* **88**, 442–443 (1981).
20. Arnold, S. J., Boksenberg, A. & Sargent, W. L. W. *Astrophys. J. Lett.* **234**, L159–L163 (1979).
21. Bonneau, D. & Foy, R. *Astr. Astrophys.* **92**, L1–L4 (1980).

Flow and instability of a viscous current down a slope

Herbert E. Huppert

Department of Applied Mathematics and Theoretical Physics, Silver Street, Cambridge CB3 9EW, UK

If viscous fluid is released on a horizontal surface it rapidly takes up a circular plan form as it spreads. This form is observed[1,2] to be stable to any small disturbances which are initiated on the front due, for example, to irregularities in the horizontal surface or to chance perturbations. Alternatively, if some fluid is released onto a sloping surface—for example, some liquid detergent on a slanted plate—a quite different plan form occurs. One, two or more extended regions of fluid develop downslope, as shown in Fig. 1*a*, *b*. A situation intermediate between these two is now discussed. Consider a broad band of viscous fluid, uniform in depth across a slope, released so as to flow down a constant slope. By following the motion, which is initially independent of the cross-slope coordinate, the speed of advance and the depth of the flow before it breaks up into a series of waves of ever increasing amplitude can be determined. I present an expression for the wavelength of the front, which is determined by surface tension and is independent of the coefficient of viscosity.

With the coordinate system depicted in Fig. 2 and use of the approximations of lubrication theory[3], the y-independent, down-slope momentum equation can be written as

$$0 = g \sin\alpha + \nu u_{zz} \tag{1}$$

In deriving equation (1) we have neglected both surface tension, the effects of which will be analysed below, and contact line effects[4], which are negligible[1] under the assumption that the Bond number $B = \rho g l^2/T \gg 1$, where ρ is the fluid density, l a representative length scale of the current and T the surface tension. Use of the equation of continuity then leads to

$$h_t + (g \sin\alpha/\nu)h^2 h_x = 0 \tag{2}$$

as the nonlinear partial differential equation for the unknown free surface $h(x, t)$. To equation (2) must be added the global continuity equation

$$\int_0^{x_N(t)} h(x, t)\mathrm{d}x = A \tag{3}$$

where $x_N(t)$ is the value of x at the front of the current and A is the initial cross-sectional area. The particular solution of equations (2) and (3) is sought in the range $0 \leq x \leq x_N(t)$.

Equation (2) shows that h is constant along characteristics given by

$$\frac{\mathrm{d}x}{\mathrm{d}t} = (g \sin\alpha/\nu)h^2 \tag{4}$$

Thus if initially $h = f(x)$, say, the equation of the characteristics is given by

$$x = x_0 + (g \sin\alpha/\nu)f^2(x_0)t \tag{5}$$

where x_0 is the initial value of the characteristic. The solution of equation (2) is thus

$$h = [\nu(x - x_0)/g \sin\alpha]^{1/2} t^{-1/2} \tag{6a}$$

$$\rightarrow (\nu/g \sin\alpha)^{1/2} x^{1/2} t^{-1/2} \qquad (x \gg x_0) \tag{6b}$$

independent of the initial conditions. When combined with equaton (3), in order to evaluate the length of the current, equation (6*b*) proves that some time after the initiation of the current, no matter what the initial shape, the solution takes the form

$$h = (\nu/g \sin\alpha)^{1/2} x^{1/2} t^{-1/2}$$
$$0 \leq x \leq x_N = (9A^2 g \sin\alpha/4\nu)^{1/3} t^{1/3} \tag{7}$$

Expressed alternatively, equation (7) represents the unique similarity solution of equations (2) and (3). The profile of the predicted current ends abruptly at $x = x_N$ with $h = h_N(t) = 1.5A/x_N$ there. The profile can be smoothed off at x_N by including the effects of surface tension. This will be done below after a discussion of an experimental investigation of the validity of the truncated profile expressed by equation (7).

Some 30 experiments were conducted using a pentagonal sheet of Perspex. The longest side was 101.7 cm and from it two sides of length 82 cm emanated at right angles. The remaining two sides were 60 cm. The sheet was surrounded by a Perspex wall 5 cm high to make a tray which was firmly attached to a rigid, flat board. Before each experiment the board was tilted by raising the 101.7-cm long side by the required amount. A removable Perspex gate was fitted 5.0 cm from the back edge of the tray and fluid poured into the space behind the gate. Three different fluids, whose physical properties are listed in Table 1, were used. After the fluid behind the gate had been left a sufficiently long time that it had become quite stationary, the gate was raised and the fluid proceeded to pour down the slope.

At first the motion was virtually independent of the cross-slope coordinate except near the walls where viscous drag retarded the flow. This form of motion is clearly evident in Fig. 1*c*. Observations of the length of the current as a function of time were taken and some typical results plotted in Fig. 3. It can be seen that the agreement between the experimental observations and the theoretical prediction (7) is good. The agreement justifies the neglect of both surface tension and contact line effects in predicting the temporal development of the two-dimensional current.

After the two-dimensional motion had continued for some time, the flow front seemed spontaneously to develop a series of small amplitude waves of fairly constant wavelength across the slope, as seen in Fig. 1*d*. The amplitude of the waves increased in time as the maxima (points furthest down the slope) travelled faster than the minima, as seen in Fig. 1*e*. The wavelength remained unaltered. The long-time shape of the flow front was different for the two fluids used. Both silicone oils developed the form shown in Fig. 1*f*. This consisted of a periodic, triangular front with tightly rounded maxima. The maxima were connected by very straight portions at an angle to the slope to extremely pointed minima. The glycerine developed the form shown in Fig. 1*g*. This was also periodic, though with much less tightly rounded maxima. These were again connected by extremely straight portions, but in this case they were almost directly down slope and connected to very broad minima.

Table 1 The fluids used, their viscosity and surface tension

Fluid	Viscosity at 17 °C ($\mathrm{cm^2 s^{-1}}$)	Surface tension at 17 °C ($\mathrm{dyn\ cm^{-1}}$)
Silicone oil MS200/100	1.15	20.6
Silicone oil MS200/1000	12.8	22.0
Glycerine	9.8	60.2

0028-0836/82/480427—03$01.00

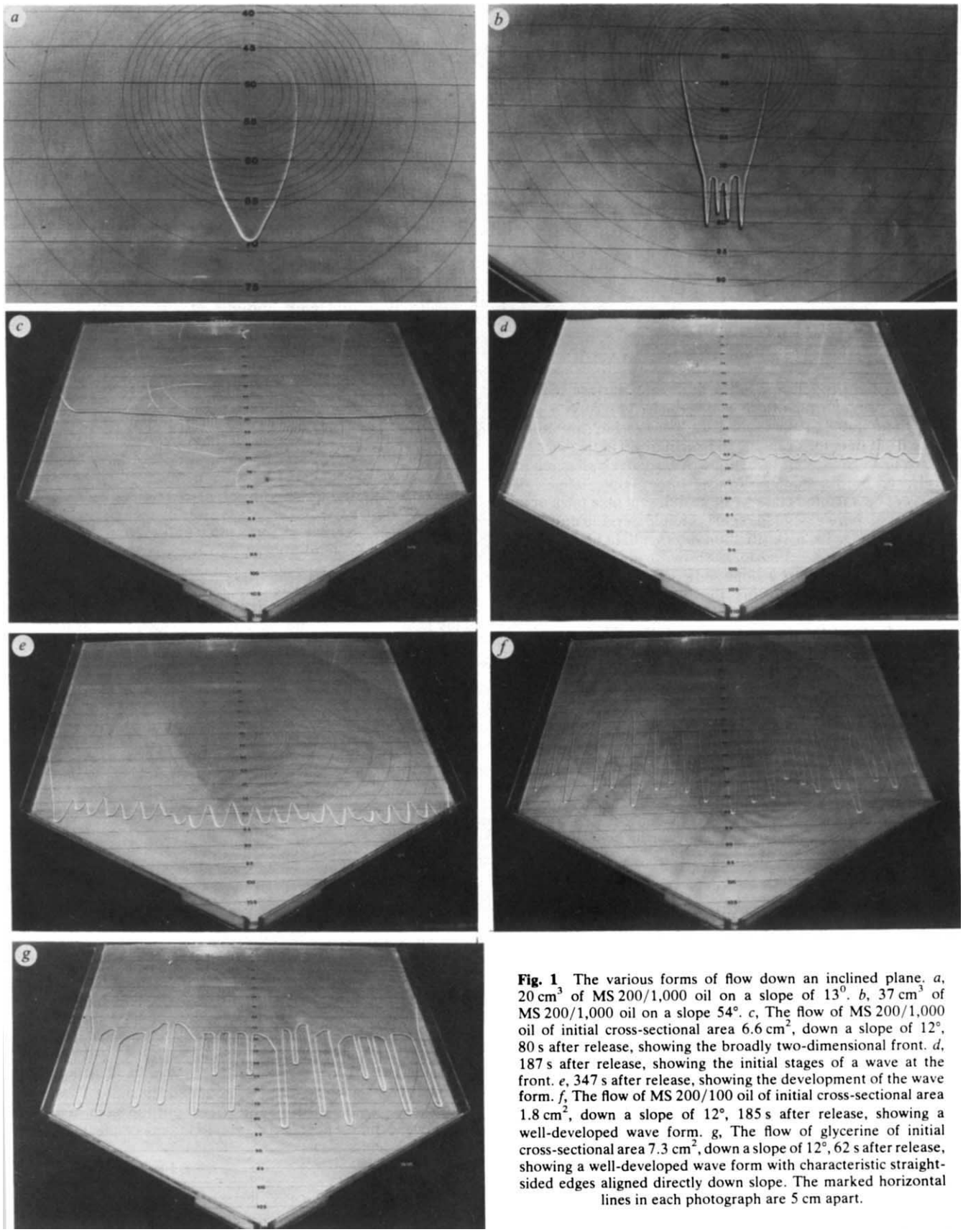

Fig. 1 The various forms of flow down an inclined plane. *a*, 20 cm^3 of MS 200/1,000 oil on a slope of 13^0. *b*, 37 cm^3 of MS 200/1,000 oil on a slope 54°. *c*, The flow of MS 200/1,000 oil of initial cross-sectional area 6.6 cm^2, down a slope of 12°, 80 s after release, showing the broadly two-dimensional front. *d*, 187 s after release, showing the initial stages of a wave at the front. *e*, 347 s after release, showing the development of the wave form. *f*, The flow of MS 200/100 oil of initial cross-sectional area 1.8 cm^2, down a slope of 12°, 185 s after release, showing a well-developed wave form. g, The flow of glycerine of initial cross-sectional area 7.3 cm^2, down a slope of 12°, 62 s after release, showing a well-developed wave form with characteristic straight-sided edges aligned directly down slope. The marked horizontal lines in each photograph are 5 cm apart.

The instability cannot be explained by viscous effects alone, since any cross-slope variation in depth of the current tends to be diminished, that is stabilized, by the cross-slope pressure gradient the variation induces. Surface tension must be taken into account.

Experiments with silicone oils whose coefficients of viscosity differ by an order of magnitude, although their surface tensions are almost equal, indicated that the wavelength of the instability is independent of the coefficient of viscosity. Experiments with the two fluids of comparable viscosity yet different surface

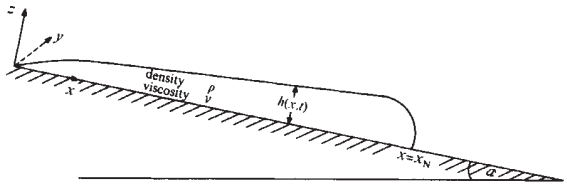

Fig. 2 A sketch of the flow and coordinate system.

tensions indicated that the wavelength is a function of the surface tension. Finally, observations taken during experiments using the same fluid but with amounts differing by up to a factor of 10 indicated that the wavelength is weakly dependent on the initial cross-sectional area A.

The form of the quasi-steady, two-dimensional tip, which is determined by including surface tension and by matching the tip onto the main flow given by equation (7), can be easily determined. The addition to equation (2) of the terms due to surface tension T leads to

$$h_t + (g \sin\alpha/\nu)h^2 h_x - 1/3(T/\rho\nu)h^3 h_{xxxx} = 0 \qquad (8)$$

In the tip the dominant balance is between the second and third terms of equation (8), the solution to which can be written as

$$h = h_N(t)H(\xi) \qquad \xi = (\rho g \sin\alpha/Th_N)^{1/3}(x_N - x) \qquad (9)$$

where $H(\xi)$ satisfies

$$H^3H''' + H^3 = 1 \qquad (10)$$

$$H \to \left(\frac{16}{15}\right)^{1/4} \xi^{3/4} \qquad (\xi \to 0) \qquad (11)$$

$$\to 1 \qquad (\xi \to \infty) \qquad (12)$$

The length scale of the tip is thus given by $(Th_N/\rho g \sin\alpha)^{1/3}$.

The experiments indicated that the instability occurs after the two-dimensional flow has propagated to a critical length X_N^C proportional to $A^{1/2}$. Evaluating the length-scale of the tip at this point and conjecturing that the wavelength, λ, is given, in scale, by this length, suggests that $\lambda \sim (A^{1/2}T/\rho g \sin\alpha)^{1/3}$. The results of the various observations, normalized in this way, are presented in Fig. 4. The data are seen to collapse together systematically with this normalization and are well represented by

$$\lambda = 7.5(A^{1/2}T/\rho g \sin\alpha)^{1/3} \qquad (13)$$

The wavelength remained constant as the amplitude of the instability increased. For the silicone oils, the distance from the origin of the furthest points down the slope increased with time like $t^{0.35}$ while the distance of the minima increased like $t^{0.28}$. For glycerine, the distance of the front of the instability, once well established, increased like $t^{0.6}$ while the minima were virtually stationary.

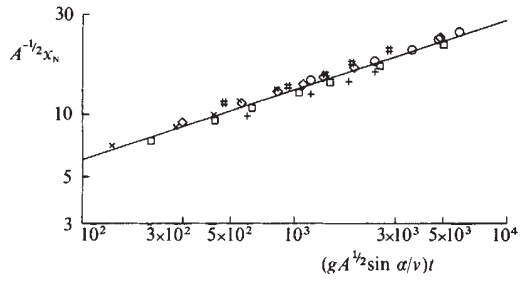

Fig. 3 The length of the two-dimensional flow, normalized with respect to $A^{1/2}$, as a functon of a suitably non-dimensional time. The straight line is the theoretical prediction obtained from equation (7). The experimental points are for values of ν, $\sin\alpha$, A in cgs units of: □, 12.9, 0.093, 8.9; ◇, 12.9, 0.20, 3.1; ○12.9, 0.65, 5.9; +, 9.8, 0.20, 9.0; ×, 9.8, 0.15, 3.6; #, 1.2, 0.11, 1.0.

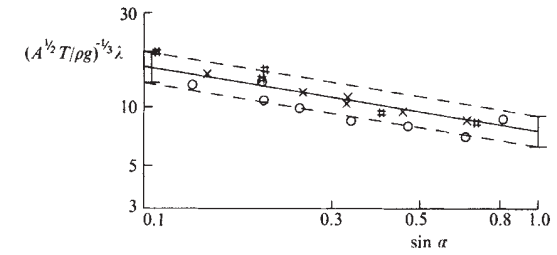

Fig. 4 The wavelength of the instability at the front, normalized with respect to $(A^{1/2}T/\rho g)^{1/3}$, as a function of the slope angle, α. Experiments with fluids of viscosities 12.9, 9.8 and 1.2 cm^2s^{-1} are plotted as ○, × and # respectively. The solid line is given by equation (14) and is the best-fit to the data. The two error bars at the end of the line represent ±15%, a typical standard deviation of the wavelength across the slope. Where two or more data points fell on top of each other all but one were omitted for the sake of clarity.

I thank E. J. Hinch for stimulating and helpful conversations, many other of my colleagues in DAMTP for useful discussions, J. M. Wheeler for experimental help and for preparation of the figures, and D. C. Cheesley, D. Lipman, G. Parker and E. J. Sharp for technical assistance.

Received 14 June; accepted 8 September 1982.

1. Huppert, H. E. *J. Fluid Mech.* **121**, 43–58 (1982).
2. Huppert, H. E. *et al. J. Volcan. Geotherm. Res.* **14** (in the press).
3. Batchelor, G. K. *An Introduction to Fluid Dynamics* (Cambridge University Press, 1967).
4. Hocking, L. M. *Q. Jl Mech. appl. Math.* **34**, 37–55 (1981).

Forces between two adsorbed polyethylene oxide layers immersed in a good aqueous solvent

Jacob Klein*† & Paul Luckham*

* Cavendish Laboratory, Madingley Road, Cambridge CB3 0HE, UK
† Polymer Department, Weizmann Institute, Rehovot, Israel

Recent measurements of the forces acting between two polystyrene layers adsorbed onto mica surfaces, immersed in a poor solvent for the polymer, show strong initial attraction as the surfaces approach, followed by ultimate repulsion[1]. This has been attributed to attractive osmotic interactions between the adsorbed layers, and possibly to the effect of bridging[2,3]. We have extended these measurements to the case of polyethylene oxide (PEO) layers adsorbed on mica, immersed in an aqueous 0.1 M KNO_3 medium at *p*H 6 (a good solvent for PEO). Using monodispersed polymer of two molecular weights, we find that an equilibrium force–distance profile is indicated. As the surfaces bearing the adsorbed PEO approach, repulsive forces commence at a surface separation $D \simeq 6 \pm 1 R_g$ (unperturbed radius of gyration of the respective polymers) and increase monotonically on approach; on subsequent separation the forces decrease monotonically to zero. We find no evidence for attraction or adhesion between the adsorbed layers in this system.

The experimental technique and procedure closely resemble those previously described[1,4]. The method permits the measurement of the force $F(D)$ acting between the mica surfaces a distance D apart, as well as the mean refractive index $n(D)$ of the medium separating them.

The forces were first determined between the bare mica surfaces in pure electrolyte. Polyethylene oxide solution was

0028–0836/82/480429—03$01.00